to erroneous results. In fact, it is unlikely that any optimization performed so far be definitive as the surface is too flat for calculations with an error range of even 1-2 kcal/mol.

Frisch et al. optimized water dimer at many different HF and MP2 calculational levels; however, it does not appear that they explored the surfaces except near to the minima found.[1d] They reported that correction for electron correlation tended to shorten the O-O distance but did not report calculations on structures resembling the trifurcated ones considered here. Clementi et al. reported minima for several water dimer structures including one containing a bifurcated H bond.[1b] They seem not to have considered structures similar to I and II, which have three H-bonding interactions.

The binding energies in Table II are reported in two ways: (a) relative to twice the lowest energy calculated for water at each level, which corresponds to the AM1-optimized geometry; and (b) relative to twice the energy of water optimized by the same procedure used to optimize the dimer. Using water optimized at the various ab initio levels used would introduce an error of 0.34-2.28 kcal/mol (twice 0.17-1.14) into the energy of two waters at the highest level used here. The common practice of comparing the dimer to waters optimized at the same level also introduces errors of the same nature for the dimer. It is not clear that these errors will always compensate for each other. It is likely that errors of this nature may apply to previously reported ab initio binding energies.

The experimental determinations of the structure[14] and binding energy[15] of the water dimer were performed at 350-400 K. On so flat a surface the free energy surface may be largely determined by entropic factors. For example, if one estimates the optimized structure to be 10 eu lower than the linear structure, at 400 K the linear structure would be favored by 4 kcal/mol from the entropic contribution to the free energy surface. This would be more than enough to render the linear structure lower in energy at the experimental temperatures.

Comparison of AM1-calculated energies with experiment poses an unusual problem for the case of water dimer. AM1 is parametrized to give enthalpies of formation at 298 K. The tacit assumption in such a system is that the optimized geometries will not differ significantly upon temperature change. As this is evidently not the case here, it is not clear whether the AM1 bonding energies should be compared with experimental bonding energies or bonding enthalpies (5.4 and 3.7 kcal/mol, respectively[13]). Curiously, the trifurcated and linear structures have AM1 bonding energies of 5.5 and 3.3 kcal/mol, respectively. Despite the imperfections of the comparisons, it is abundantly clear that AM1 does give interaction energies that are within reason. This is particularly important for more complex systems where other geometrical constraints preclude the possibility of forming three H bonds between water molecules.

Conclusion

Both AM1 and high-level ab inito calculations appear to lead to structures of reasonable energy for the water dimer. That the "optimized" structures differ significantly in geometry seems to be more the result of the flatness of the surface than of any fundamental inadequacies of the AM1 methodology. In fact, AM1 optimization leads to the best structures for monomeric water and (constrained) linear water dimer. A structure qualitatively similar to the overall AM1 minimum is negligibly higher in energy than the best dimer considered in this study.

Acknowledgment. This work was supported in part by a PSC-CUNY grant.

Supplementary Material Available: Table of calculated 6-311G** energies (hartrees) (1 page). Ordering information is given on any current masthead page.

(14) Dyke, T. R.; Mack, K. M.; Muenter, J. S. *J. Chem. Phys.* **1977**, *66*, 498.

(15) Curtiss, L. A.; Frurip, D. J.; Blander, M. *J. Chem. Phys.* **1979**, *71*, 2703.

Thermalization Distances and Times for Subexcitation Electrons in Solid Water

T. Goulet and J.-P. Jay-Gerin*

Groupe du Conseil de Recherches Médicales du Canada en Sciences des Radiations et Département de Médecine Nucléaire et de Radiobiologie, Faculté de Médecine, Université de Sherbrooke, Sherbrooke, Québec, Canada J1H 5N4 *(Received: May 31, 1988; In Final Form: September 7, 1988)*

We report the results of our Monte Carlo simulations of the thermalization of subexcitation electrons in solid water. The electron scattering cross sections used in the calculations were those recently determined by Michaud and Sanche from slow-electron-impact experiments on thin amorphous ice films. We find an average electron thermalization distance of about 13 nm, which is larger than what is usually assumed (~2-7 nm) in models describing diffusion-controlled track reactions in irradiated liquid water. Our calculated average thermalization time is $\sim 10^{-13}$ s, in good agreement with experimental observations. The possibility for the subexcitation electrons to undergo a dissociative attachment to water molecules was also considered. We show that this process could explain the unscavengeable initial yield of molecular hydrogen.

Introduction

Over the past three decades, much effort has been devoted to the study of the interaction of ionizing radiation with liquid water since this substance is the chief constituent of biological matter. As proposed by Platzman,[1] the succession of events that accompanies the passage of ionizing radiation through a medium may be divided into the physical, the physicochemical, and the chemical stages. For liquid water, the physical stage ($\lesssim 10^{-15}$ s) is well described by sophisticated Monte Carlo codes[2-4] which simulate the "histories" of both the incident particles and the numerous secondary electrons produced by ionization. During the physicochemical stage, from about 10^{-15} to 10^{-12} s, the $^{\bullet}H_2O^{+}$ ions react

(1) Platzman, R. L. *The Vortex* **1962**, *23*, 372.

(2) Hamm, R. N.; Wright, H. A.; Ritchie, R. H.; Turner, J. E.; Turner, T. P. In *Proceedings of the Fifth Symposium on Microdosimetry, Verbania-Pallanza, 22-26 Sept. 1975*; Report No. EUR 5452; Booz, J., Ebert, H. G., Smith, B. G. R., Eds.; Commission of the European Communities: Luxembourg, 1976; p 1037.

(3) Malbert, M.; Carel, C.; Patau, J. P.; Terrissol, M. In *Seventh Symposium on Microdosimetry, Oxford, 8-12 Sept. 1980*; Report No. EUR 7147; Booz, J., Ebert, H. G., Hartfiel, H. D., Eds.; Harwood Academic: London, 1981; p 359.

(4) Zaider, M.; Brenner, D. J.; Wilson, W. E. *Radiat. Res.* **1983**, *95*, 231.

0022-3654/88/2092-6871$01.50/0

with the surrounding H_2O molecules while the excited neutral molecules, H_2O^*, may dissociate. During this interval, the subexcitation electrons (those which have fallen below the energy threshold for electronic excitations, i.e., ~7.4 eV)[5] lose their excess energy, thermalize, and become trapped and subsequently hydrated.[6-9] The species formed at $\sim 10^{-12}$ s ($^{\bullet}OH$, e_{aq}^-, $^{\bullet}H$, H_3O^+, H_2, $^{\bullet}O^{\bullet}$)[10] then begin to diffuse and to react with each other. This diffusion-controlled chemical development of the track through later times corresponds to the chemical stage. Because of the track structure of the initial spatial distribution of chemical species, the chemical stage involves nonhomogeneous kinetics[11] and the reaction rates depend on the initial positions of the species. It is therefore of primary importance to know the distribution of thermalization distances of the subexcitation electrons, a quantity which has been shown to play a crucial role in the decay kinetics of many chemical species.[12-14]

Up to now, the greatest difficulty encountered in studying subexcitation electrons has been the paucity of data concerning their interaction with molecules in the condensed phase. Recently, however, Michaud and Sanche[15] have determined the scattering cross sections of low-energy (~1-20 eV) electrons in solid H_2O from electron-impact experiments on thin amorphous ice films at 14 K. The aim of the present study is to use these new electron-scattering cross sections in an attempt to determine the distributions of thermalization distances and times for subexcitation electrons in condensed water. Since Michaud and Sanche[15] worked with films of amorphous ice, we expect to find distributions whose characteristics are more representative of liquid water than of crystalline ice. In this work, we also investigate the possibility that a subexcitation electron undergoes a dissociative attachment to a water molecule, and the consequences of such a process on the initial yields of various chemical species.

Calculations

With respect to the bottom of the solid water conduction band, the lowest electron energy considered in Michaud and Sanche's cross-section data[15] is ~2.7 eV, assuming the conduction-band edge of amorphous ice to lie at $V_0 \cong -1$ eV below vacuum.[16,17] These cross sections quantify the relative probabilities of the elastic and the various inelastic (inter- and intramolecular vibrations) scattering processes that an excess slow electron may undergo in solid H_2O. They are also accompanied by a coefficient of angular anisotropy which gives a simple description of the angular distribution of a scattering event.[15] Since no data exist for electron energies below ~2.7 eV, we estimated the cross sections in this energy region by taking the electron mean free path of ~0.5 nm at near zero energy calculated by Neff et al.,[18] and by interpolating linearly the cross sections between ~0 and 2.7 eV. The angular distribution of the scattering events at these very low energies was assumed to be described by the same coefficient of angular anisotropy as that given by Michaud and Sanche[15] at ~2.7 eV.

In order to provide a full stochastic treatment of the thermalization process of subexcitation electrons in solid water, our earlier Monte Carlo electron transport code[19] was adapted to simulate the situation where an electron, generated at the origin of a coordinate system with a given initial kinetic energy $E_0 \lesssim 7.4$ eV, migrates in a random-walk fashion and transfers progressively its excess energy to the medium until it gets thermalized. The distribution function $P_{E_0}(R)$ of radial distances traveled by the electrons in thermalizing from E_0 was calculated by averaging R over a large number (~300 000) of electron histories. The corresponding distribution function $P_{E_0}(t)$ of electron thermalization times was calculated simultaneously in the same manner.

Typical functions $P_{E_0}(R)$ and $P_{E_0}(t)$ obtained for $E_0 = 3$ eV are shown in Figures 1 and 2. $P_{E_0}(R)$ was found to be well described by the (normalized) function

$$f(R) = \frac{2^{1/2}}{\pi^{1/2} b^3} R^2 \exp(-R^2/2b^2) \qquad (1)$$

where b is the dispersion parameter. The average electron thermalization distances $\langle R \rangle$ and times $\langle t \rangle$ obtained for different values of E_0 are given in Table I with the corresponding values of b. It is worth noting that our calculated $\langle R \rangle$ values for $E_0 < 2.5$ eV are in excellent agreement with the experimental ther-

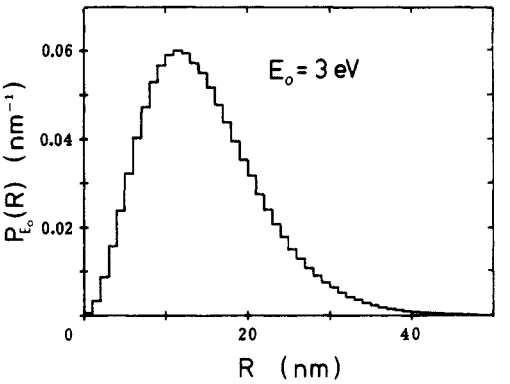

Figure 1. Distribution function $P_{E_0}(R)$ of radial distances traveled by 3-eV electrons in thermalizing from E_0 in solid water.

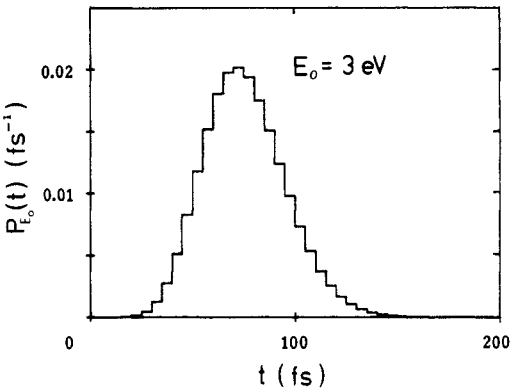

Figure 2. Distribution function $P_{E_0}(t)$ of times spent by 3-eV electrons in thermalizing from E_0 in solid water.

TABLE I: Variation of the Average Electron Thermalization Distance and Time with Initial Electron Kinetic Energy in Solid H_2O

E_0, eV	$\langle t \rangle$, fs	$\langle R \rangle$, nm	b,[a] nm	P_{diss}[b]
7.2	198.1	38.4	23.8	0.303
6.5	184.7	36.5	22.6	0.245
5.5	160.0	32.6	20.1	0.101
4.5	129.6	26.9	16.5	0.008
3.5	93.1	18.8	11.5	
2.5	56.9	9.8	6.0	
1.5	33.6	4.9	3.0	
0.5	17.9	2.5	1.5	

[a] Dispersion parameter obtained from a fit of $f(R)$ to $P_{E_0}(R)$ (see text). [b] Probability that a subexcitation electron undergoes reaction 3.

(5) Platzman, R. L. *Radiat. Res.* **1955**, *2*, 1.
(6) Mozumder, A.; Magee, J. L. *Int. J. Radiat. Phys. Chem.* **1975**, *7*, 83.
(7) Turner, J. E.; Magee, J. L.; Wright, H. A.; Chatterjee, A.; Hamm, R. N.; Ritchie, R. H. *Radiat. Res.* **1983**, *96*, 437.
(8) Wiesenfeld, J. M.; Ippen, E. P. *Chem. Phys. Lett.* **1980**, *73*, 47.
(9) Migus, A.; Gauduel, Y.; Martin, J. L.; Antonetti, A. *Phys. Rev. Lett.* **1987**, *58*, 1559.
(10) See, for example: Klassen, N. V. In *Radiation Chemistry: Principles and Applications*; Farhataziz, Rodgers, M.A.J., Eds.; VCH: New York, 1987; Chapter 2, p 29.
(11) Freeman, G. R. *Annu. Rev. Phys. Chem.* **1983**, *34*, 463.
(12) Fanning, Jr., J. E.; Trumbore, C. N.; Barkley, P. G.; Short, D. R.; Olson, J. H. *J. Phys. Chem.* **1977**, *81*, 1026.
(13) Burns, W. G.; May, R.; Buxton, G. V.; Tough, G. S. *Faraday Discuss. Chem. Soc.* **1977**, *63*, 47.
(14) Zaider, M.; Brenner, D. J. *Radiat. Res.* **1984**, *100*, 245.
(15) Michaud, M.; Sanche, L. *Phys. Rev. A* **1987**, *36*, 4672, 4684.
(16) Baron, B.; Hoover, D.; Williams, F. *J. Chem. Phys.* **1978**, *68*, 1997.
(17) Grand, D.; Bernas, A.; Amouyal, E. *Chem. Phys.* **1979**, *44*, 73.
(18) Neff, H.; Sass, J. K.; Lewerenz, H. J.; Ibach, H. *J. Phys. Chem.* **1980**, *84*, 1135.
(19) Goulet, T.; Jay-Gerin, J.-P.; Patau, J. P. *J. Electron Spectrosc. Relat. Phenom.* **1987**, *43*, 17.

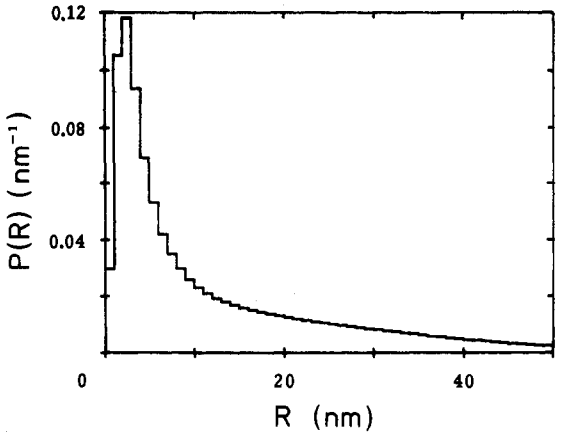

Figure 3. Distribution function $P(R)$ of radial thermalization distances for all subexcitation electrons ($E_0 \lesssim 7.4$ eV) in solid water, taking account of their energy spectrum $D(E_0)$ given by eq 2.

malization lengths of photoinjected subexcitation electrons in liquid water recently reported by Konovalov et al.[20] This agreement, in turn, greatly strengthens the credibility of our treatment of the cross sections in this energy region.

In order to average $\langle R \rangle$ and $\langle t \rangle$ over all possible initial electron energies E_0, a knowledge of the energy spectrum of the subexcitation electrons is required. For water (in the vapor or liquid phase), Kaplan and Miterev[21] have recently shown that the energy distribution function $D(E_0)$ of subexcitation electrons is very similar to that found for helium, provided an appropriate scaling is made to account for the different values of the lowest electronic excitation energy. Using the calculated spectra of Platzman[5] and Douthat[22] for helium, we thus adopted here the spectral distribution function

$$D(E_0) = \frac{0.053}{7.4} + \frac{181.2}{(E_0 + 8.3)^3}, \quad E_0 \lesssim 7.4 \text{ eV} \qquad (2)$$

Since we allowed for a possible dissociative attachment of the subexcitation electrons to water molecules, some of the electrons do not get thermalized. In fact, attributing all the so-called "other energy losses" of Michaud and Sanche[15] to the following resonant dissociative electron attachment process

$$e^- + H_2O \rightarrow H_2O^- \rightarrow H^- + {}^\bullet OH \qquad (3)$$

yields a proportion of subexcitation electrons undergoing reaction 3 which varies from 30.3% for $E_0 = 7.2$ eV to 0% for $E_0 < 4.2$ eV (see Table I). Using these proportions and the subexcitation spectrum of eq 2, we found that 97% of the electrons in the subexcitation energy range do not undergo the dissociative attachment but instead become thermalized with an average thermalization distance $\overline{\langle R \rangle} = 12.8$ nm and an average thermalization time $\overline{\langle t \rangle} = 68$ fs. The resulting spatial distribution function $P(R)$ for all the thermalized electrons is shown in Figure 3. As we can see, $P(R)$ differs significantly from the function $f(R)$ which adequately fitted the distribution functions $P_{E_0}(R)$. A satisfactory representation of $P(R)$ could nevertheless be obtained by using a sum of four such $f(R)$ functions with different values of b, namely,

$$P(R) \simeq \sum_{i=1}^{4} a_i f_i(R) \qquad (4)$$

where $a_1 = 0.1953$, $b_1 = 1.27$ nm, $a_2 = 0.2691$, $b_2 = 2.59$ nm, $a_3 = 0.2242$, $b_3 = 6.27$ nm, $a_4 = 0.3114$, and $b_4 = 17.35$ nm.

Discussion

Our calculated electron thermalization distance distribution can be characterized by two values: (i) the most probable value of R, equal to 2.5 nm, and (ii) the average thermalization distance $\overline{\langle R \rangle} = 12.8$ nm. The difference between these two values comes from the long tail of the distribution which indicates that a number of electrons travel relatively large distances from subexcitation to thermal energies. Our value of $\overline{\langle R \rangle}$ is larger than the thermalization lengths usually quoted in the literature for liquid water which are in the range ~2–7 nm.[6,7,13,14,23–27]

The value of 68 fs obtained for the average thermalization time is somewhat larger than the $\sim 2 \times 10^{-14}$ s time scale recently proposed by Mozumder[28] for electron thermalization in liquid water. Our $\overline{\langle t \rangle}$ value, however, is smaller than the observed formation time of the hydrated electron at room temperature ($\sim 3 \times 10^{-13}$ s).[6–9] An interesting comparison can also be made with the recent femtosecond experiments of Migus et al.[9] which indicate that a ~1.5-eV electron initially produced by photoionization of water at 21 °C gets trapped in about 110 fs. This trapping time is longer than our calculated electron thermalization time $\langle t \rangle \cong 34$ fs for $E_0 = 1.5$ eV (see Table I). Although important uncertainties exist in both these calculated and experimental times, the difference between the two values seems to support Mozumder's conjecture that thermalization precedes trapping in liquid water.[28]

A few words should finally be said about the dissociative electron attachment process which we included in our simulations. Although this process is well established in the vapor phase,[29–31] it has only recently been observed in solid water by electron-stimulated desorption experiments.[32] In high-pressure gases, and probably in the condensed phase, the hydride ions formed according to reaction 3 react with the surrounding water molecules via the very fast proton-transfer process

$$H^- + H_2O \rightarrow H_2 + OH^- \qquad (5)$$

with a reaction rate constant of $\sim 10^{12}$ M^{-1} s^{-1}.[33,34] It is worth mentioning that reactions 3 and 5 do not significantly affect the yields of e_{aq}^- and $^\bullet OH$ since we found that only ~3% of the subexcitation electrons give rise to the formation of $^\bullet OH$, H_2, and OH^- through the dissociation of two H_2O molecules. This proportion of 3% is in remarkable agreement with the observed ratio $G_{H_2}/(G_{e_{aq}^-} + G_{H_2})$, where G_{H_2} and $G_{e_{aq}^-}$ are the initial yields of H_2 (~ 0.016 μmol J^{-1})[25] and of e_{aq}^- (~ 0.50 μmol J^{-1}),[10] respectively. Our results thus give a quantitative support to the hypothesis that reactions 3 and 5 are responsible for the unscavengeable initial yield of molecular hydrogen in water radiolysis.[35,36]

The present study calls for further investigation on three points. First, it would be desirable to determine with more accuracy both the electron scattering cross sections in condensed H_2O at energies below ~2.7 eV, and the energy distribution of subexcitation electrons. Second, it would be interesting to examine how our calculated electron thermalization distance distribution would affect the modeling of the diffusion-controlled kinetics of the various chemical species produced during water radiolysis. Finally, the simulations should be modified to include the Coulomb attraction between the positive parent ion and the associated ejected electron and to account for a possible recombination of the opposite charges prior to the completion of the thermalization.

(20) Konovalov, V. V.; Raitsimring, A. M.; Tsvetkov, Yu. D. *Radiat. Phys. Chem.* **1988**, *32*, 623.
(21) Kaplan, I. G.; Miterev, A. M. In *Advances in Chemical Physics*; Prigogine, I., Rice, S. A., Eds.; Wiley: New York, 1987; Vol. LXVIII, p 255.
(22) Douthat, D. A. *Radiat. Res.* **1975**, *61*, 1.
(23) Kuppermann, A. In *Radiation Research, Proceedings of the Third International Congress of Radiation Research, Cortina d'Ampezzo, June–July 1966*; Silini, G., Ed.; North-Holland: Amsterdam, 1967; p 212.
(24) Mozumder, A. *J. Chem. Phys.* **1969**, *50*, 3153.
(25) Schwarz, H. A. *J. Phys. Chem.* **1969**, *73*, 1928.
(26) Trumbore, C. N.; Short, D. R.; Fanning, Jr., J. E.; Olson, J. H. *J. Phys. Chem.* **1978**, *82*, 2762.
(27) Magee, J. L.; Chatterjee, A. *Radiat. Phys. Chem.* **1980**, *15*, 125.
(28) Mozumder, A. *Radiat. Phys. Chem.* **1988**, *32*, 287.
(29) Schulz, G. J. *J. Chem. Phys.* **1960**, *33*, 1661.
(30) Compton, R. N.; Christophorou, L. G. *Phys. Rev.* **1967**, *154*, 110.
(31) Melton, C. E. *J. Chem. Phys.* **1972**, *57*, 4218.
(32) Sanche, L.; Parenteau, L., to be submitted for publication.
(33) Stockdale, J. A. D.; Compton, R. N.; Reinhardt, P. W. *Phys. Rev. Lett.* **1968**, *21*, 664.
(34) Melton, C. E.; Neece, G. A. *J. Am. Chem. Soc.* **1971**, *93*, 6757.
(35) Platzman, R. L. In *Abstracts of Papers*, Second International Congress of Radiation Research, Harrogate, 5–11 Aug. 1962; p 128.
(36) Faraggi, M.; Désalos, J. *Int. J. Radiat. Phys. Chem.* **1969**, *1*, 335.

Acknowledgment. We thank M. Michaud, L. Parenteau, and L. Sanche for providing us information about their experimental results, M. Inokuti for valuable discussions, and D. Hunting and S. Lang for a critical reading of the manuscript. We are also indebted to C. Houée-Levin for pointing out the relevance of the initial yield of H_2 to this study. Financial support from the Medical Research Council of Canada, the Ministère de l'Enseignement Supérieur et de la Science du Québec, and the Natural Sciences and Engineering Research Council of Canada is gratefully acknowledged.

Proton Mobility in Liquid and Frozen $HClO_4 \cdot 5.5H_2O$: NMR and Conductivity Measurements

T.-H. Huang,* R. A. Davis,

School of Physics, Georgia Institute of Technology, Atlanta, Georgia 30332

U. Frese,† and U. Stimming

Department of Chemical Engineering and Applied Chemistry, Columbia University, New York, New York 10027 *(Received: June 28, 1988; In Final Form: October 3, 1988)*

^2H NMR spectra and conductivity of liquid and frozen $HClO_4 \cdot 5.5H_2O$ have been obtained over the temperature range of 140–300 K. The ^2H NMR spectra show a gradual broadening of an isotropic resonance at lower temperature from $\Delta\nu_{1/2}$ = 2 Hz at ~300 K to ~50 kHz at 170 K. At even lower temperatures, flat-top spectra of breadth ~170 kHz were observed. The presence of isotropic spectra above 170 K indicates that the deuterons (protons) are relatively mobile even in the frozen state. A plot of ln $(1/\Delta\nu_{1/2})$ vs $(1/T)$, the Arrhenius plot, further reveals the presence of two phase transitions centered at 228 ± 2 and 180 ± 5 K. Conductivity measurements agree well with the NMR results. The activation energies were determined from NMR (conductivity) measurements to be 0.27 eV (0.29 eV) from 228 to 180 K and 0.40 eV (0.36 eV) from 180 to 140 K.

Introduction

In normal aqueous electrochemistry the temperature can be varied roughly between −15 and 95 °C. This small temperature range severely limits the investigation of the temperature dependence of electrochemical processes. In particular, it prevents an experimental test of quantum-mechanical theories of electron-transfer reactions and the determination of the contribution of tunneling processes at low temperature.[1] In recent studies it has been shown that the investigation of processes at the metal–aqueous electrolyte interface can be extended to temperatures below the freezing point of the electrolyte, and it has been demonstrated for reactions as well as double-layer properties.[1-3] The electrolyte that has been used in these investigations is aqueous perchloric acid of the composition $HClO_4 \cdot 5.5H_2O$. In the phase diagram of H_2O–$HClO_4$ this composition represents an acid hydrate of a stoichiometric composition with the highest water content possible. The freezing point of that compound is 228 K. Recently the crystal structure of $HClO_4 \cdot 5.5H_2O$ was determined by Mootz et al.[4,5] using X-ray diffraction. According to Mootz and Wiebke[4] the compound crystallizes in a clathrate structure, similar to several gas hydrates, of the cubic 12-Å type. H_2O and H^+ form the host lattice while ClO_4^- is the guest. At temperatures $T < 173$ K a higher order phase transformation seems to take place which is reversible upon going back to higher temperatures.

Since perchloric acid hydrate is a suitable electrolyte also in the frozen state, it was assumed that the protons are relatively mobile even in the solid phase. In order to clarify this point, NMR and conductivity measurements were performed to obtain some insight into the proton mobility of $HClO_4 \cdot 5.5H_2O$ at various temperatures in the liquid and frozen states of the electrolyte.

Experimental Section

The conductivity measurements were performed using an ac bridge technique (1 kHz) and fast galvanostatic pulses. Detailed analysis of impedance experiments at various frequencies yielded essentially the same results as obtained at 1 kHz. The fast galvanostatic pulse technique does only give the resistance, and a calibration was used to obtain conductivity values. The cell consisted of two platinum foils, each of approximately 2-cm^2 area, which were positioned approximately 1 mm apart from each other. The cell is similar to the one described earlier[3] and had a temperature accuracy of approximately ±2 K. Measurements were performed in an aqueous solution of $HClO_4$ (ACS grade) which corresponds to the composition of the 5.5 hydrate. Measurements were not performed in deuteriated solutions. The difference between H^+ and D^+ was not considered crucial for this preliminary study. The conductivity was measured as a function of temperature from higher to lower temperatures and vice versa.

Deuterium NMR quadrupolar spectra were obtained on a home-built 300-MHz spectrometer (^2H frequency 46 MHz) interfaced to a Nicolet 1280 computer data system with 293B pulse programmer and a 2090 transient recorder capable of digitizing up to 2 MHz at 12 bit resolution. Spectra without proton decoupling were obtained using either a single pulse sequence for temperatures above 190 K where T_2, the spin–spin relaxation time, is long, or quadrupolar echo technique[6] for temperatures below 190 K ($P_{\pi/2} = 2$ μs). The spectra obtained with the two methods were indistinguishable at temperatures near 190 K. However, no attempt was made to compare the intensity loss. Recycle delay

† Current address: Institute of Physical Chemistry, University of Bonn, D-5300 Bonn 1, West Germany.

(1) Stimming, U.; Schmickler, W. *J. Electroanal. Chem.* **1983**, *150*, 125.
(2) Frese, U.; Stimming, U. *J. Electroanal. Chem.* **1986**, *198*, 409.
(3) Dinan, T.; Stimming, U. *J. Electrochem. Soc.* **1986**, *133*, 2662.
(4) Wiebcke, M.; Mootz, D. *Z. Kristallogr.* **1985**, *170*, 194.
(5) Mootz, D.; Oellers, E. J.; Wiebcke, M. *J. Am. Chem. Soc.* **1987**, *109*, 1200.
(6) Davis, J. H.; Jeffrey, K. P.; Bloom, M.; Valic, M. F.; Higgs, T. P. *Chem. Phys. Lett.* **1976**, *42*, 390.
(7) Huang, T.-H.; Skarjune, R. P.; Wittebort, R. J.; Griffin, R. G.; Oldfield, E. *J. Am. Chem. Soc.* **1980**, *102*, 7377.
(8) Wittebort, R. J.; Olejniczak, E. T.; Griffin, R. G. *J. Chem. Phys.* **1987**, *86*, 5411.

0022-3654/88/2092-6874$01.50/0